

## Article

# Electro-Hydraulic Servo-Pumped Active Disturbance Rejection Control in Wind Turbines for Enhanced Safety and Accuracy

Tiangui Zhang <sup>1</sup>, Haohui Yu <sup>1</sup>, Bo Yu <sup>1,2,\*</sup>, Chao Ai <sup>1</sup>, Xiaoxiang Lou <sup>3</sup>, Pengjie Xiang <sup>4</sup>, Ruilin Li <sup>5</sup> and Jianchen Li <sup>5</sup>

<sup>1</sup> School of Mechanical Engineering, Yanshan University, Qinhuangdao 066004, China; tianguiz@stumail.ysu.edu.cn (T.Z.); pinggushechuan@163.com (H.Y.); aichao@ysu.edu.cn (C.A.)

<sup>2</sup> Mechanical and Electrical Engineering, Xinjiang Institute of Engineering, Urumqi 830023, China

<sup>3</sup> Ningbo Anson CNC Technique Co., Ltd., Ningbo 315000, China; 15221668844@139.com

<sup>4</sup> School of Automation Science and Electrical Engineering, Beihang University, Beijing 100191, China; pjxiang@buaa.edu.cn

<sup>5</sup> Shenzhen Inovance Technology Co., Ltd., Shenzhen 518000, China; liruilin@inovance.com (R.L.); lijianchen@inovance.com (J.L.)

\* Correspondence: yub@stumail.ysu.edu.cn; Tel.: +86-0991-7977157

**Abstract:** Aiming at the high accuracy and high robustness position control of servo pump control in the pitch system of a wind turbine generator, this paper proposes an active disturbance rejection controller (ADRC). The ADRC considers pitch angular velocity and acceleration limits. According to the kinematics principle of the pump-controlled pitch system, the relationship between the pitch angular velocity and acceleration limit and the displacement of the hydraulic cylinder is established. Through the method of theoretical analysis, the nonlinear relationship expression between pitch angle and hydraulic cylinder displacement is obtained, and the linearization of pitch angular velocity control is realized; the formula for  $b_0$  (the estimated value of the input gain of the system) of the pump-controlled pitch system is obtained by the method of modeling and analysis,  $b_0$  is the key parameter for the design of the ADRC; the stability of the controller parameters is proved through the stability analysis and simulation analysis, and the design of the self-immobilizing controller with pitch angular velocity and acceleration limitation is the completed ADRC design. Finally, a joint simulation platform of AMESim and MATLAB as well as a physical experiment platform of electro-hydraulic servo pump-controlled pitch control is constructed, and the effectiveness of the proposed control method is verified through simulation and experiment. The results show that compared with the unrestricted ADRC and PID, the velocity-acceleration-limited ADRC can effectively improve the control effect of the angular velocity and acceleration of the paddle, smooth the startup process, improve the safety of the system, and have better position control accuracy and anti-jamming ability.

**Keywords:** ADRC; electro-hydraulic servo pump-controlled; pitch angle control; wind turbine



**Citation:** Zhang, T.; Yu, H.; Yu, B.; Ai, C.; Lou, X.; Xiang, P.; Li, R.; Li, J. Electro-Hydraulic Servo-Pumped Active Disturbance Rejection Control in Wind Turbines for Enhanced Safety and Accuracy. *Processes* **2024**, *12*, 908. <https://doi.org/10.3390/pr12050908>

Academic Editor: Krzysztof Rogowski

Received: 12 March 2024

Revised: 25 April 2024

Accepted: 25 April 2024

Published: 29 April 2024



**Copyright:** © 2024 by the authors. Licensee MDPI, Basel, Switzerland. This article is an open access article distributed under the terms and conditions of the Creative Commons Attribution (CC BY) license (<https://creativecommons.org/licenses/by/4.0/>).

## 1. Introduction

Large wind turbines utilize pitch-control technology to achieve reliable power regulation [1]. Electro-hydraulic servo systems are commonly employed in pitch systems for their better power density and various benefits [2–6]. At present, the wind turbine pitch control system mainly uses two forms of electro-hydraulic servo devices: servo valve control and servo pump control. Servo valve control is a more traditional program; the basic principle is to control the opening of the servo valve, adjust the oil supply, and then drive the hydraulic cylinder piston movement, to achieve the adjustment of the pitch angle. Although the servo valve is compact and has a fast response speed, there are some inherent defects, such as control accuracy by the internal friction and leakage, and energy efficiency is low [7–11]. In contrast, servo pump control is a more advanced and energy-saving technology route. In this program, the variable pump directly drives the hydraulic cylinder through the control of the pump displacement to adjust the output flow and pressure and then to control the pitch angle. Due to the elimination of the throttle

valve, the oil circuit is more simple, and the energy loss is greatly reduced. At the same time, the servo pump control also has high control accuracy and good dynamic response, and adaptability, as well as other advantages making it especially suitable for wind power generation, such as reliability and the environmental adaptability of the application of high requirements [12–15].

The servo pump-controlled pitch system is a typical nonlinear system [16–19], the multi-source and time-varying nature of the load makes the system's working conditions uncertain, and the flow nonlinearity of the hydraulic pump, the internal oil compression and leakage of the system, and other factors affect the system's position control accuracy [20–23]. At the same time, the hydraulic cylinder and pitch-angle movement are in a nonlinear relationship; focusing only on the hydraulic cylinder movement does not guarantee the safety of the pitch control system, and the need for pitch-angle speed and acceleration is also limited. Therefore, the study of high-precision position control of an electro-hydraulic servo pump-controlled pitch system considering the pitch-angle motion limitation has important engineering application value.

Singh V.P. et al. looked into the stable performance of a closed-circuit hydrostatic actuator using a variable-displacement pump and a variable-displacement motor. They assessed the actuator's overall performance by taking into account the efficiencies of the pump, motor, and drive pump, and derived equations to describe the drive efficiency [24]. Anwar M.N. and colleagues introduced a proportional-integral (PI) controller for pitch-angle control to reduce the time delay from the hydraulic system. The controller is designed using a direct synthesis method to get the desired response [25]. Kou Fairong and colleagues examined how the motor affects the system force, developed a Linear-Quadratic-Gaussian (LQG) controller, and suggested a current controller based on the inner-loop motor speed to achieve force-tracking control, enhancing the dynamic properties of the pump-controlled system [26]. Wu X. et al. utilized a self-learning asymmetric support vector machine (ASVM) approach to detect internal leakage in the hydraulic pitch system of the pump-controlled pitch system. This method was confirmed by NREL's Fast [27]. Gu Yajing introduced a direct-drive hydraulic pump-controlled motor pitch system to address the issues of high energy consumption and complex control mechanisms in traditional pitch systems. This system utilizes an adaptive backstepping controller based on the backstepping technique and adaptive algorithms to achieve precise pitch control and enhance the stability of the unit's power output [28]. Li Bin and colleagues conducted research on high-performance pitch-control technology for large wind turbines. They applied an electro-hydraulic servo-pump-controlled pitch-control system to address issues with load perturbation and poor system robustness. They utilized a fuzzy PID control strategy to enhance the system's overall anti-interference performance [29].

Currently, many scholars have researched the nonlinear and high-precision position control of pump control systems. However, few scholars have integrated the unique operational characteristics of wind turbine pitch with the safety standards of the pitch motion process and nonlinear control. In order to improve the pitch-angle position-control accuracy, compensate for the rapid fluctuation of wind speed as well as other internal and external nonlinear factors of the system, and ensure the robustness of the system, this paper adopts the ADRC strategy for control. ADRC is a kind of modern control strategy, and the core idea of this control method is to dynamically estimate and compensate for the internal and external disturbances of the system. It is characterized by simple structure, easy implementation, and low requirements for model accuracy and strong robustness. It is suitable for complex systems with high model uncertainty and large changes in external environment, and can effectively improve the performance and stability of the system. According to the kinematics principle of the pump-controlled pitch system, the relationship between the pitch angular velocity and acceleration limit and the displacement of the hydraulic cylinder is established. Through the method of theoretical analysis, the nonlinear relationship expression between pitch angle and hydraulic cylinder displacement is obtained, and the linearization of pitch angular velocity control is realized; the method of modeling analysis is used to obtain the calculation formula of  $b_0$  of the pump-controlled

pitch system, and the key parameters are determined for the design of the ADRC; the stability of the controller parameters is proved through the stability analysis and simulation analysis, and the design of a self-immobilizing controller with pitch angular velocity and acceleration limitation is the completed ADRC design. The control effect was studied on the experimental platform. The experimental results show that the designed controller takes the speed variance of pitch angle as the velocity stability index. Compared with unlimited ADRC, there was a 98.38% increase in pitch-angle stability; pitch-angle acceleration is always controlled within the prescribed  $20 \text{ deg/s}^2$ ; by analyzing the displacement variance of pitch angle, the limited ADRC improved the accuracy of position by 94.1% versus PID. The control method can improve the control accuracy and safety of the system.

## 2. Principle of Electro-Hydraulic Servo Pump-Controlled Pitch System

The electro-hydraulic servo-pump-controlled pitch system comprises a permanent magnet synchronous servo motor, hydraulic pump, electromagnetic directional valve, single throttle valve, relief valve, check valve, throttle valve, accumulator, hydraulic cylinder, blade wheels, and sensors. The host computer determines the desired pitch angle based on the current pitch angle and wind speed data. It then converts this desired pitch angle into a command for the hydraulic cylinder displacement. This command is executed by the servo motor to control the flow and pressure of the hydraulic pump, which in turn adjusts the paddles to achieve the desired pitch angle through the hydraulic cylinder. Figure 1 below illustrates the hydraulic mechanism of the servo pump-controlled pitch system of the wind turbine.

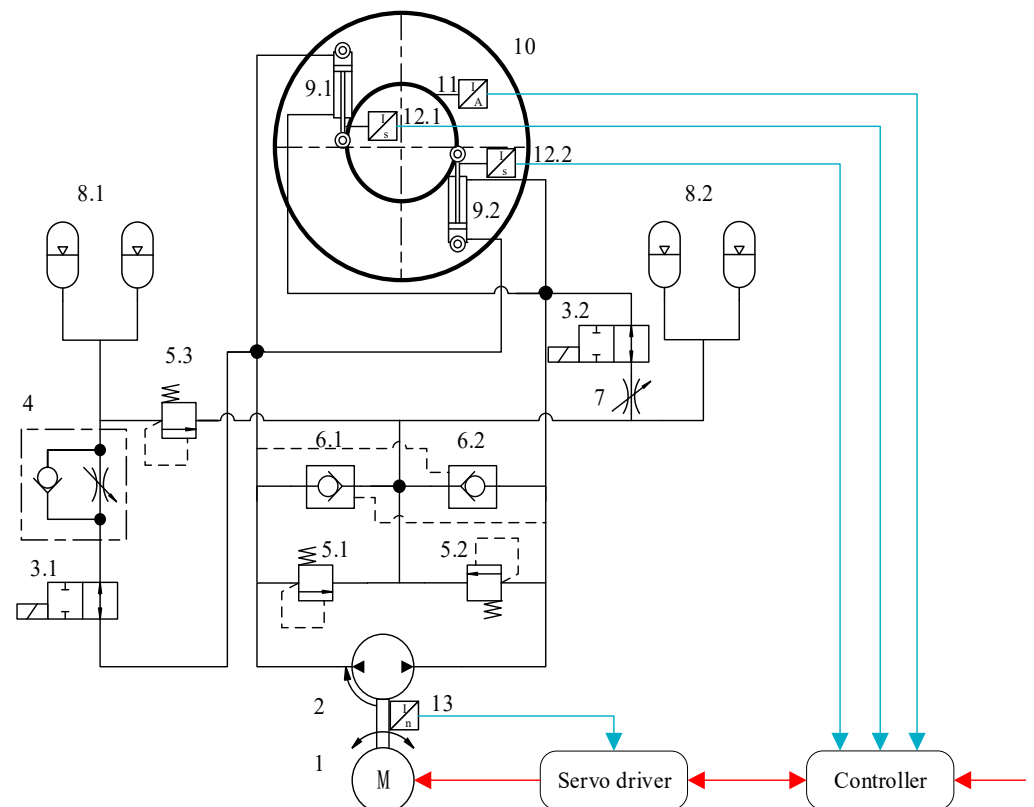


**Figure 1.** Hydraulic principle of servo-pump-controlled pitch system for wind turbine generator: 1—permanent magnet synchronous servo motor; 2—hydraulic pump; 3—electromagnetic directional valve; 4—single throttle valve; 5—relief valve; 6—check valve; 7—throttle valve; 8—accumulator; 9—hydraulic cylinder; 10—blade wheels; 11—angle sensor; 12—position sensor; 13—revolution sensor.

### 3. Kinematic Analysis of Pitch Mechanism

To secure the pitch system safe, it is essential to define the correlation between the hydraulic cylinder and the pitch angle to restrict the hydraulic cylinder's motion in pitch control. The analyzing process is as follows.

The hydraulic cylinder of the pitch system is attached to the hub and the blade through hinging mechanisms. Pitch control is achieved by extending or retracting the piston rod of the hydraulic cylinder. Figure 2 displays the schematic diagram of the pitch mechanism.

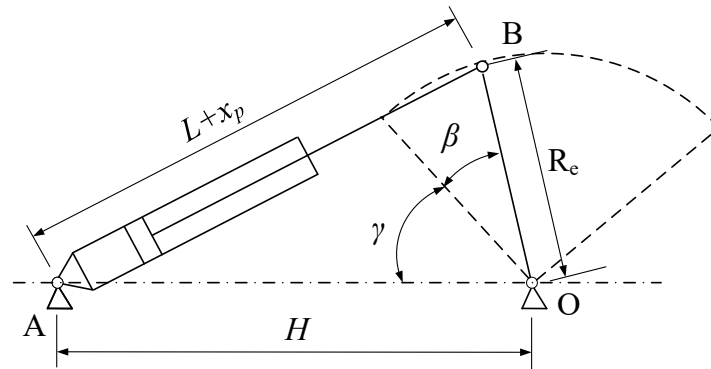


**Figure 2.** Schematic diagram of pitch mechanism.

$L$  represents the fully retracted length of the hydraulic cylinder,  $x_p$  is the displacement of the hydraulic cylinder,  $R_e$  is the hub's radius of rotation,  $H$  is the distance between the hydraulic cylinder body's articulation point and the paddle's rotation axis,  $\gamma$  is the mounting angle, and  $\beta$  is the pitch angle.

Assuming the hydraulic cylinder, piston rod, connecting rod, etc. are rigid bodies without elastic deformation, the relationship between  $x_p$  and  $\beta$  can be described using the principle of pitch mechanism.

$$\beta = \arccos \left[ \frac{R_e^2 + H^2 - (L + x_p)^2}{2R_e H} \right] - \gamma \quad (1)$$

The pitch-angle velocity  $\dot{\beta}$  can be expressed as:

$$\dot{\beta} = \frac{(L + x_p) \dot{x}_p}{R_e H \sqrt{1 - \left[ \frac{R_e^2 + H^2 - (L + x_p)^2}{2R_e H} \right]^2}} \quad (2)$$

The pitch-angle acceleration  $\ddot{\beta}$  can be expressed as:

$$\ddot{\beta} = \frac{(L + x_p) \ddot{x}_p + \dot{x}_p^2}{R_e H \sqrt{1 - \left( \frac{R_e^2 + H^2 - (L + x_p)^2}{2R_e H} \right)^2}} - \frac{4(L + x_p)^2 \dot{x}_p^2 (R_e^2 + H^2 - (L + x_p)^2)}{R_e^3 H^3 \left( 4 - \frac{(R_e^2 + H^2 - (L + x_p)^2)^2}{R_e^2 H^2} \right)^{\frac{3}{2}}} \quad (3)$$

Table 1 shows the specific dimensions of the pitch mechanism. Bringing the numerical value into Formulas (2) and (3), the hydraulic cylinder and pitch-angle motion diagram is shown in Figure 3.

**Table 1.** Specific dimensions of pitch mechanism.

| H      | $R_e$   | L     | $\gamma$ |
|--------|---------|-------|----------|
| 1.75 m | 0.625 m | 1.5 m | 56.633°  |

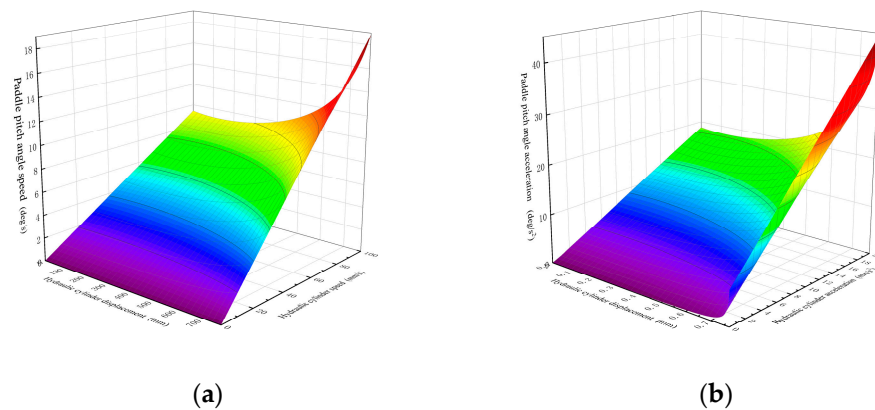


**Figure 3.** Relationship between hydraulic cylinder and pitch angle. (a) The hydraulic cylinder displacement, hydraulic cylinder velocity, and pitch-angle velocity curve; (b) The relation curve of hydraulic cylinder displacement, hydraulic cylinder acceleration, and pitch-angle acceleration.

As can be seen from Figure 3a, there is an approximate linear relationship between the angle velocity of the pitch and the displacement of the hydraulic cylinder in the first half of the hydraulic cylinder movement, but the nonlinear phenomenon between the angle velocity of the pitch and the displacement of the hydraulic cylinder is very serious when the hydraulic cylinder moves to the second half. It can be seen from Figure 3b that the pitch-angle acceleration and hydraulic cylinder displacement of the motion of the relationship between the first half of the hydraulic cylinder is approximately linear; in the hydraulic cylinder movement to the second half, the nonlinear phenomenon is very serious. Since the wind turbine pitch system is a large inertia system, too fast a motion will affect the stability of the system, to ensure the safety of the pitch control system, the pitch-angle speed and acceleration need to be limited. In the experience of wind power developers and operators, the pitch-angle speed limit to 5 deg/s, and the acceleration limit to 20 deg/s<sup>2</sup>.

Transforming Equations (2) and (3), The equation that describes the relationship between hydraulic cylinder displacement and velocity for the pitch-angle velocity limit is:

$$v_{pLimit} = \frac{\dot{\beta}_{max} R_e H \sqrt{1 - \left[ \frac{R_e^2 + H^2 - (L + x_p)^2}{2R_e H} \right]^2}}{L + x_p} \quad (4)$$

where  $v_{pLimit}$  is the hydraulic cylinder limiting speed and  $\dot{\beta}_{max}$  is the pitch-angle limiting speed.

The hydraulic cylinder displacement, velocity, and acceleration relationship equation for pitch-angle acceleration limitation is:

$$a_{pLimit} = \frac{\ddot{\beta}_{max} R_e H \sqrt{1 - \left( \frac{R_e^2 + H^2 - (L + x_p)^2}{2R_e H} \right)^2} - \dot{x}_p^2 + \frac{\dot{x}_p^2 (L + x_p)^2 (R_e^2 + H^2 - (L + x_p)^2)}{2R_e^2 H^2 \left( 1 - \left( \frac{R_e^2 + H^2 - (L + x_p)^2}{2R_e H} \right)^2 \right)}}{L + x_p} \quad (5)$$

where  $a_{pLimit}$  is the hydraulic cylinder limiting acceleration and  $\ddot{\beta}_{max}$  is the pitch-angle limiting acceleration.

#### 4. Modeling of Electro-Hydraulic Servo-Pump-Controlled Pitch System

ADRC design does not require high accuracy in the model; unmodeled components are observed by the observer as an expanded state for feedforward compensation. However, there is a crucial parameter in feedforward compensation: the estimated system input gain,  $b_0$ , which must initially be determined as an approximate value when designing the controller. The precision of  $b_0$  does not need to be very high, thus the system modeling

does not overly consider factors with low influence weights, and higher-order terms are generally neglected.

The load flow equation for a hydraulic pump can be expressed as:

$$Q_p = D_p \omega_m - C_{ip}(P_1 - P_r) - C_{ep}P_1 \quad (6)$$

When the effective volume of the two chambers of the hydraulic cylinder is equal, the flow continuity equation for the high pressure chamber of the hydraulic cylinder is:

$$Q_p = A_{p1}\dot{x}_p + C_{tc}P_1 + \frac{V_t}{2\beta_e}\dot{P}_1 \quad (7)$$

The load force balance equation for a hydraulic cylinder is:

$$A_{p1}P_1 - A_{p2}P_r = M_t\ddot{x}_p + B_p\dot{x}_p + Kx_p + F_L \quad (8)$$

$Q_p$  is the output flow rate of hydraulic pump,  $D_p$  is the displacement of hydraulic pump,  $\omega_m$  is the speed of servo motor,  $C_{ip}$  is the internal leakage coefficient of hydraulic pump,  $C_{ep}$  is the external leakage coefficient of hydraulic pump,  $P_1$  is the pressure of high pressure chamber of hydraulic pump,  $P_r$  is the pressure of low pressure chamber of hydraulic pump,  $A_{p1}$  is the effective area of rod-less chamber of hydraulic cylinder,  $x_p$  is the displacement of piston of hydraulic cylinder,  $C_{tc}$  is the total leakage coefficient of hydraulic cylinder,  $V_t$  is the effective volume of hydraulic cylinder, and  $\beta_e$  is the modulus of elasticity of hydraulic fluid.  $A_{p2}$  is the effective area of the rod cavity of the hydraulic cylinder,  $M_t$  is the equivalent mass of the piston and load of the hydraulic cylinder,  $B_p$  is the viscous damping coefficient of the piston and load,  $K$  is the spring stiffness of the load, and  $F_L$  is the friction and external load interference force.

A Laplace transform of Equations (6)–(8) yields:

$$Q_p = D_p \omega_m - C_{tp}P_1 \quad (9)$$

$$Q_p = A_{p1}x_p s + C_{tc}P_1 + \frac{V_t}{2\beta_e}P_1 s \quad (10)$$

$$A_{p1}P_1 = M_t x_p s^2 + B_p x_p s + Kx_p + F_L \quad (11)$$

where  $C_{tp}$  is the total leakage coefficient of the hydraulic pump,  $C_{tp} = C_{ip} + C_{ep}$ .

Collating (9)–(11) gives:

$$x_p = \frac{D_p \omega_m - \left( \frac{V_t}{2\beta_e A_{p1}} s + \frac{K_c}{A_{p1}} \right) F_L}{\frac{V_t M_t}{2\beta_e A_{p1}} s^3 + \left( \frac{K_c M_t}{A_{p1}} + \frac{V_t B_p}{2\beta_e A_{p1}} \right) s^2 + \left( A_{p1} + \frac{K_c B_p}{A_{p1}} + \frac{V_t K}{2\beta_e A_{p1}} \right) s + \frac{K_c K}{A_{p1}}} \quad (12)$$

where  $K_c$  is the total leakage coefficient of the hydraulic pump and cylinder,  $K_c = C_{ip} + C_{ep} + C_{tc}$ .

When  $\frac{K_c B_p}{A_{p1}} \ll A_{p1}$  and  $K = 0$ , Equation (12) can be written as:

$$x_p = \frac{\frac{D_p}{A_{p1}} \omega_m - \frac{K_c}{A_{p1}^2} \left( \frac{V_t}{2\beta_e K_c} s + 1 \right) F_L}{s \left[ \frac{V_t M_t}{2\beta_e A_{p1}^2} s^2 + \left( \frac{K_c M_t}{A_{p1}^2} + \frac{V_t B_p}{2\beta_e A_{p1}^2} \right) s + 1 \right]} \quad (13)$$

Take the system state vector  $x = [x_1, x_2]^T = [x_p, \dot{x}_p]^T$ , the system input vector  $u = \omega_m$ , consider the 3rd order term as a perturbation, take the position and velocity of the hydraulic cylinder as the system state variables and the servomotor output rotational speed as the

system input variable, and the system state space expression in the following form can be derived from Equation (13):

$$\begin{cases} \dot{x}_1 = x_2 \\ \dot{x}_2 = \frac{-\frac{V_t M_t}{2\beta_e A_{p1}^2} \ddot{x}_2 - x_2 - \frac{V_t}{2\beta_e A_{p1}^2} \dot{F}_L - \frac{K_c}{A_{p1}^2} F_L + \frac{D_p}{A_{p1}} u}{\frac{K_c M_t}{A_{p1}^2} + \frac{V_t B_p}{2\beta_e A_{p1}^2}} \\ y = x_1 \end{cases} \quad (14)$$

Express  $\dot{x}_2$  as a 3-term, then the nonlinear part of the system is:

$$f(x_1, x_2) = \frac{-\frac{V_t M_t}{2\beta_e A_{p1}^2} \ddot{x}_2 - x_2}{\frac{K_c M_t}{A_{p1}^2} + \frac{V_t B_p}{2\beta_e A_{p1}^2}} \quad (15)$$

Out-of-system load disturbances are:

$$w(t) = -\frac{\frac{V_t}{2\beta_e A_{p1}^2} \dot{F}_L(t) + \frac{K_c}{A_{p1}^2} F_L(t)}{\frac{K_c M_t}{A_{p1}^2} + \frac{V_t B_p}{2\beta_e A_{p1}^2}} \quad (16)$$

The system input gain estimate is:

$$b_0 = \frac{\frac{D_p}{A_{p1}}}{\frac{K_c M_t}{A_{p1}^2} + \frac{V_t B_p}{2\beta_e A_{p1}^2}} \quad (17)$$

Equation (14) can be written as:

$$\begin{cases} \dot{x}_1 = x_2 \\ \dot{x}_2 = f(x_1, x_2) + w(t) + b_0 u \\ y = x_1 \end{cases} \quad (18)$$

From the above modeling analysis, a general expression for  $b_0$  is obtained, and a second-order nonlinear state space expression for the electro-hydraulic servo pump control system is established. By substituting parameters according to different specifications of the electro-hydraulic servo systems, the value of  $b_0$  can be determined.

## 5. Pitch Angular Velocity and Acceleration Limited ADRC Design

ADRC comprises a Tracking Differentiator (TD), Expanded State Observer (ESO), and Nonlinear State Error Feedback (NLSEF). The TD facilitates a smooth transition process for trajectory planning. The ESO conducts real-time tracking estimation and compensation for uncertain nonlinear factors, as well as internal and external disturbances in the controlled system, to enhance the system's anti-disturbance capability and positional accuracy. The NLSEF integrates error signals to create a unified control law [30–32]. Figure 4 displays the structure of ADRC.

In this paper, in order to achieve the pitch angular velocity and acceleration limiting requirements of the pitch system, and at the same time, to cope with the rapid changes and other internal and external disturbances, and to prevent the overshooting or instability of the pitch-angle control, ADRC is used for the pitch control. The pitch angular velocity and angular acceleration limiting link is introduced in the TD. When the wind speed fluctuation causes the pitch angular velocity or acceleration to be too large, the limiting link will automatically smooth the command signal to prevent the pitch mechanism from exceeding the physical constraints or causing mechanical vibration. Adopting nonlinear ESO, all internal and external disturbances are observed as a whole and treated as an expansion

state. For the nonlinear factors such as sudden change of wind speed and internal leakage, ESO quickly estimates the estimated total perturbation and compensates the estimated total perturbation by timely feedback to the controller output link to realize the active offset of the perturbation. In this way, no matter how the wind speed changes, what the controlled object “sees” is always a linearized model after the perturbation is canceled, which avoids overshooting and instability. The fal function is introduced in the NLSEF module, which has stronger nonlinear toughness than the linear feedback, and can suppress the oscillation of the pitch response caused by the wind speed perturbation and improve the stability margin of the system.

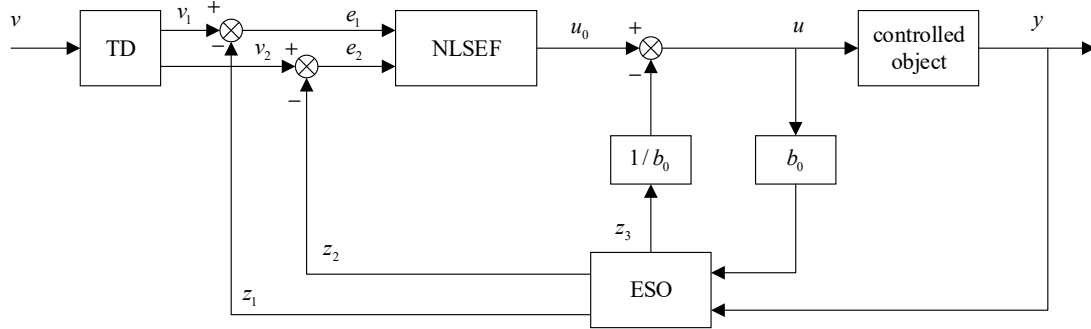


Figure 4. ADRC structure.

5.1. Nonlinear TD Design for Velocity and Acceleration Limiting

Defining the target displacement as v and substituting Equation (4) into the nonlinear TD, the nonlinear TD with speed limit can be obtained:

$$\begin{cases} \dot{v}_1 = v_2 \\ \dot{v}_2 = fhan(v_1 - v, v_2, r_0, h_0) \\ v_2 \leq v_{pLimit} \end{cases} \tag{19}$$

where  $v_1$  is the first-order tracking signal,  $v_2$  is the second-order tracking signal,  $h_0$  is the filtering factor,  $r_0$  is the tracking speed, and  $fhan(v_1 - v, v_2, r_0, h_0)$  is the integrated function of the maximum speed control of the discrete system, whose algorithmic formula is as follows:

$$\begin{cases} d = r_0 h \\ d_0 = h d \\ y = x_1 + h x_2 \\ a_0 = \sqrt{d^2 + 8 r_0 |y|} \\ a = \begin{cases} x_2 + \frac{(a_0 - d)}{2} \text{sign}(y), & |y| > d_0 \\ x_2 + \frac{y}{h}, & |y| \leq d_0 \end{cases} \\ fhan = - \begin{cases} r_0 \text{sign}(a), & |a| > d \\ r_0 \frac{a}{d}, & |a| \leq d \end{cases} \end{cases} \tag{20}$$

In Equation (19), given the target command v, the first-order tracking signal  $v_1$  will converge to the target command according to the size of the second-order tracking signal  $v_2$ , and the tracking speed  $r_0$  determines whether the second-order tracking signal  $v_2$  changes quickly or slowly, so the physical significance of  $v_1$  is the displacement of hydraulic cylinder, the physical significance of  $v_2$  is the speed of hydraulic cylinder, and the physical significance of  $r_0$  is the acceleration of hydraulic cylinder, so  $r_0$  can be taken according to the Equations (4) and (5); therefore, it can be taken according to the formula, so as to realize the acceleration limitation of the variable pitch system, namely:

$$r_0 = a_{pLimit} \tag{21}$$

Nonlinear TD with velocity and acceleration limits:

$$\begin{cases} \dot{v}_1 = v_2 \\ \dot{v}_2 = f_{han}(v_1 - v, v_2, a_{pLimit}, h) \\ v_2 \leq v_{pLimit} \end{cases} \quad (22)$$

By arranging the transition process through Equation (22), it is possible to change the linear displacement of the hydraulic cylinder to a nonlinear displacement, so as to realize the linear motion of the pitch angle, and at the same time, to realize the speed limitation and variable acceleration limitation of the pitch angle, so as to improve the smoothness and safety of the system.

### 5.2. ESO Design

Expanding the state variables of the system in Equation (18) by taking  $x_3 = f(x_1, x_2, w(t))$ , the state space equation of the system can be written as:

$$\begin{cases} \dot{x}_1 = x_2 \\ \dot{x}_2 = x_3 + b_0 u \\ \dot{x}_3 = f(x_1, x_2, w(t)) \\ y = x_1 \end{cases} \quad (23)$$

Establishment ESO:

$$\begin{cases} e = z_1 - y \\ \dot{z}_1 = z_2 - \beta_{01} e \\ \dot{z}_2 = z_3 - \beta_{02} fal(e, \alpha_1, \delta) + b_0 u \\ \dot{z}_3 = -\beta_{03} fal(e, \alpha_2, \delta) \end{cases} \quad (24)$$

where  $z_i$  is the observed value of the system output  $x_i$  ( $i = 1, 2$ ) and the total system disturbance  $x_3$ ,  $\beta_{0i}$  is the adjustable parameter of the ESO, and  $i = 1, 2, 3$ .

Where  $fal(e, \alpha_2, \delta)$  is a nonlinear function with the following expression:

$$fal(e, \alpha, \delta) = \begin{cases} \frac{e}{\delta^{1-\alpha}}, & |e| \leq \delta \\ |e|^\alpha \text{sign}(e), & |e| \geq \delta \end{cases} \quad (25)$$

where  $\alpha$  is the adjustable parameter;  $\delta$  is the length of the linear interval of the fal function.

The role of ESO is to estimate and compensate the internal and external disturbances of the system in real time, which plays a very important role in the system, in order to ensure the convergence of ESO, the following demonstrates the stability of ESO with the given parameters.  $\beta_{01} = 100, \beta_{02} = 540, \beta_{03} = 1920, \alpha_1 = 0.25, \alpha_2 = 0.75, \delta = 0.05$ .

First, check whether matrix  $K_1$  is a Hurwitz matrix.

$$K_1 = \begin{bmatrix} \beta_{01} & 1 & 0 \\ \beta_{02} & 0 & 1 \\ \beta_{03} & 0 & 0 \end{bmatrix} = \begin{bmatrix} 100 & 1 & 0 \\ 540 & 0 & 1 \\ 1920 & 0 & 0 \end{bmatrix} \quad (26)$$

The characteristic polynomial of this matrix is:

$$\det(sI - K_1) = s^3 + 100s^2 + 540s + 1920 \quad (27)$$

According to the Routh–Hurwitz stability criterion, all the roots of the polynomial lie in the left half-plane of the complex plane; therefore, the matrix  $K_1$  is a Hurwitz matrix.

Next, the Lyapunov function  $V_\theta(z)$  is chosen, and it is verified that its derivatives are negatively definite along the vector field  $F(z)$ .

$$V_\theta(z) = \sum_{i=1}^3 V_{i\theta}(z_i) \quad (28)$$

where,

$$V_{i0}(z_i) = z_i^T P_i z_i, P_i \quad (29)$$

Satisfies the Lyapunov equation

$$A_i^T P_i + P_i A_i = -I \quad (30)$$

$$A_1 = A_2 = A_3 = \begin{bmatrix} 0 & 1 & 0 \\ 0 & 0 & 1 \\ -\beta_{01} & -\beta_{02} & -\beta_{03} \end{bmatrix} \quad (31)$$

Solve the Lyapunov equation to obtain  $P_1, P_2, P_3$ .

$$P_1 = P_2 = P_3 = \begin{bmatrix} 0.0190 & 0.0017 & -0.0003 \\ 0.0017 & 0.0052 & -0.0001 \\ -0.0003 & -0.0001 & 0.0010 \end{bmatrix} \quad (32)$$

These matrices are symmetric and positive definite, satisfying the Lyapunov equation. Therefore,  $V_\theta(z)$  is positive definite.

Next, the derivative of  $V_\theta(z)$  along  $F(z)$  is calculated.

$$F(z) = [F_1(z_1)^T, F_2(z_2)^T, F_3(z_3)^T]^T \quad (33)$$

where,

$$F_{ij}(z_i) = z_{i(j+1)} - \beta_{i(j-1)} \text{fal}(z_{i1}, \alpha_j, \delta), j = 1, 2 \quad (34)$$

$$F_{i3}(z_i) = -\beta_{i2} \text{fal}(z_{i1}, 1, \delta) \quad (35)$$

$$\frac{\partial V_\theta}{\partial z} \cdot F(z) = \sum_{i=1}^3 \left[ \frac{\partial V_{i0}}{\partial z_i} \cdot F_i(z_i) \right] \quad (36)$$

It follows from the fact that

$$\frac{\partial V_1(\theta)}{\partial z_1} \cdot F_1(z_1) = -z_{11}^2 - (\beta_{01} z_{11} - z_{12})^2 - (\beta_{02} z_{11} - z_{13})^2 - \beta_{03}^2 z_{11}^2 \quad (37)$$

is negatively definite, each  $\frac{\partial V_{i0}}{\partial z_i} \cdot F_i(z_i)$  is negatively definite, and hence the derivative of  $V_\theta(z)$  is negatively definite along  $F(z)$ .

This proves the asymptotic stability of the dilation state vector  $z$ . According to Theorem II. 1 of [33], there exist  $\theta^* \in (0, 1)$  and  $r^* > 1$  such that when  $\theta \in (\theta^*, 1)$  and  $r \in (r^*, \infty)$ , the ESO error converges and the closed-loop system state is consistently bounded. It has been proven above that the designed ESO is asymptotically stable and the observation error converges to zero at an exponential rate by Lyapunov stability theory according to the given parameters. Meanwhile, the closed-loop system state is consistently bounded. This proves the effectiveness and stability of the ESO design.

### 5.3. NLSEF Design

Based on the outputs of the TD and the ESO, the error between the desired and feedback values of the system and its differential signals are calculated. The NLSEF is obtained by nonlinearly weighting the state error and combining it with the observed value of the total system perturbation  $z_3$ , to obtain the output control quantity of the ADRC  $u$ .

$$u = u_0 - \frac{z_3}{b_0} \quad (38)$$

Substituting Equation (38) into the state space expression of the system gives:

$$\begin{cases} \dot{x}_1 = x_2 \\ \dot{x}_2 = f(x_1, x_2, w(t)) + b_0 \left( u_0 - \frac{z_3}{b_0} \right) \\ y = x_1 \end{cases} \quad (39)$$

Since  $z_3$  is the observed value of the total system disturbance  $x_3$ , there is  $z_3 = x_3$  in case the observed state is accurate, so the system state space expression can be simplified as:

$$\begin{cases} \dot{x}_1 = x_2 \\ \dot{x}_2 = b_0 u_0 \\ y = x_1 \end{cases} \quad (40)$$

Design NLSEF:

$$\begin{cases} e_1 = v_1 - z_1 \\ e_2 = v_2 - z_2 \\ u_0 = \beta_1 fal(e_1, a_1, \delta) + \beta_2 fal(e_2, a_2, \delta) \end{cases} \quad (41)$$

where  $a_i$  is the adjustable parameter,  $i = 1, 2$ ;  $\beta_i$  is the control gain,  $i = 1, 2$ .

After the above derivation, the ADRC for pitch system with pitch-angle velocity and acceleration limits is obtained and its structure is shown in Figure 5.

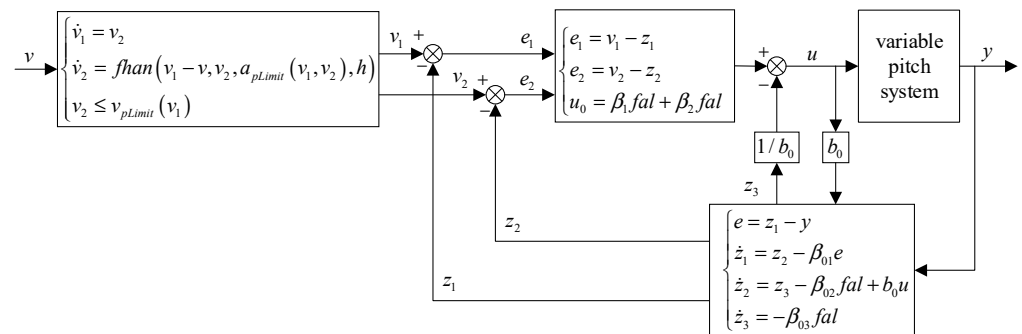


Figure 5. ADRC for speed and acceleration limiting.

The ESO and TD are designed to incorporate speed and acceleration limits for the pitch mechanism in order to coordinate the control of hydraulic cylinder position and speed. This ensures that the signals produced by the TD remain within the safety parameters of the pitch system, preventing excessive speed or acceleration during signal tracking.

## 6. Experimental Research

A joint simulation platform is built in AMESim (2020.1) and MATLAB (R2021a) software to simulate the working state of the pump-controlled pitch system. A comparison test between an ADRC with speed and acceleration limitation and an ADRC without speed and acceleration limitation is carried out to verify the effectiveness of speed and acceleration limitation. The advantages of the ADRC with speed and acceleration limitation in position control accuracy are verified by comparing the control effects of PID control and ADRC with speed and acceleration limitation. An experimental platform of electro-hydraulic servo-pump-controlled pitch system is also built to physically verify the effectiveness of the self-resistant controller with pitch angular velocity and acceleration limitation.

### 6.1. Software Simulation

The joint simulation platform of AMESim and MATLAB for electro-hydraulic servo pump-controlled pitch system was built, as shown in Figure 6.

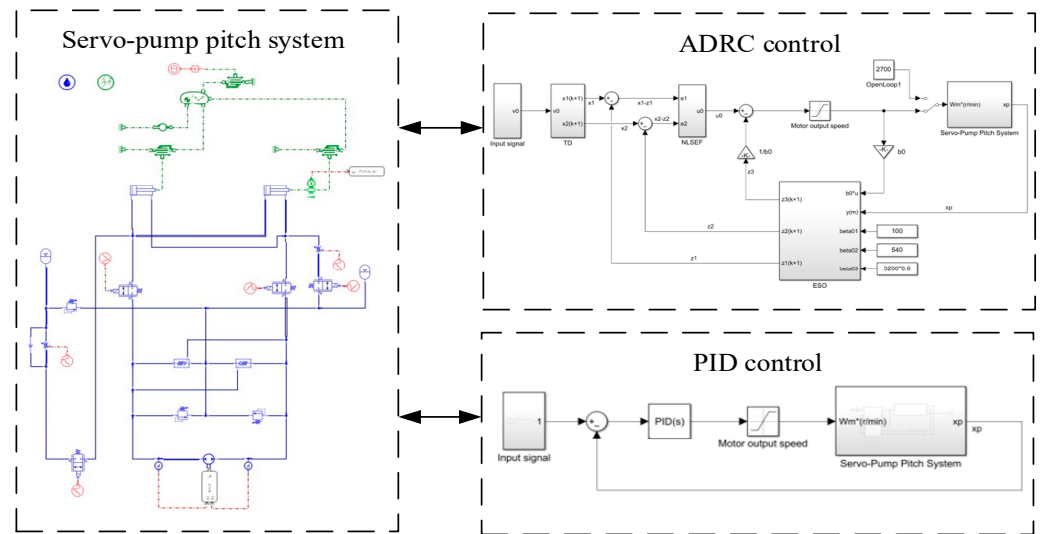


**Figure 6.** The joint simulation platform of AMESim and MATLAB for electro-hydraulic servo-pump-controlled pitch system.

The ADRC parameters are shown in Table 2.

**Table 2.** Parameters of the ADRC section.

| Parameter Name            | Numerical Value | Parameter Name            | Numerical Value |
|---------------------------|-----------------|---------------------------|-----------------|
| Speed of transition $r_0$ | $a_pLimit$      | Filtering factor $h_0$    | 0.05            |
| ESO gain $\beta_{01}$     | 100             | Control volume gain $b_0$ | 0.79            |
| ESO gain $\beta_{02}$     | 540             | NLSEF gain $\beta_1$      | 220             |
| ESO gain $\beta_{03}$     | 1920            | NLSEF gain $\beta_2$      | 44              |

In order to compare the control effect of ADRC and PID for speed and acceleration limitation, according to the maximum outstretched displacement of 800 mm of the pitch hydraulic cylinder as the target command, the parameters of PID are adjusted against the response time of ADRC, so that the PID arrives at the target position without overshooting. The effect is shown in Figure 7.

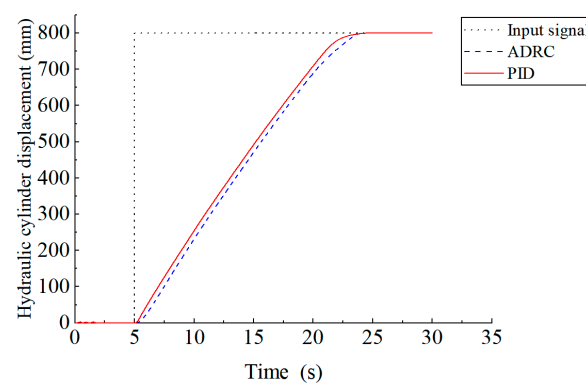


**Figure 7.** The outstretched displacement of 800 mm of the pitch hydraulic cylinder.

Both ADRC and PID reach the target value at 23 s. The corresponding PID parameters are P of 180, I of 0, and D of 20.

### 6.2. Study on the Effect of ADRC Control for Velocity-Acceleration Limitation

#### 6.2.1. Simulation Study of Speed Limiting Effect of ADRC

Experiments on the effect of displacement and velocity control with unrestricted ADRC are carried out and the results are shown in Figure 8.

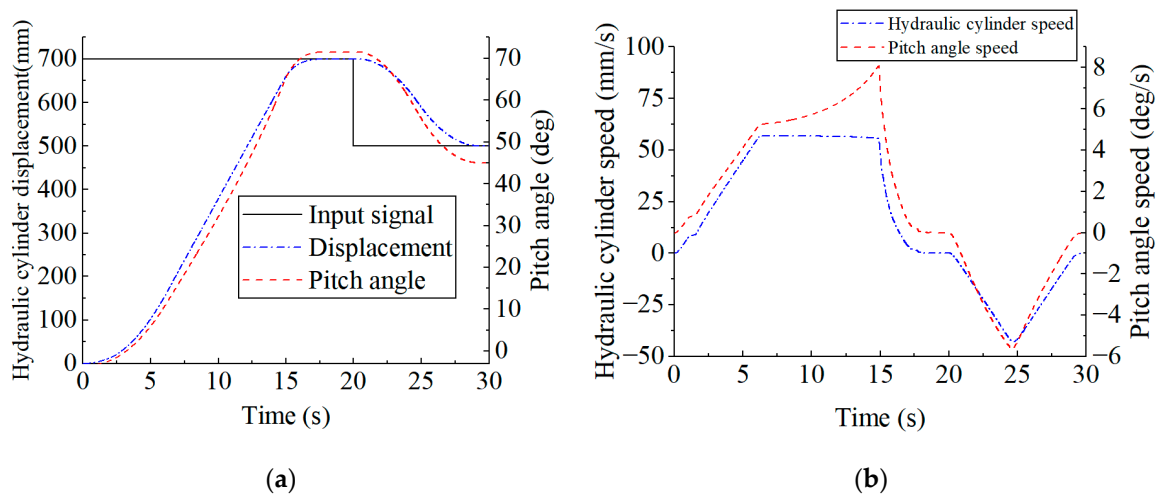


**Figure 8.** Displacement and velocity control with unrestricted ADRC: (a) Hydraulic cylinder displacement and pitch-angle control with unrestricted ADRC; (b) Hydraulic cylinder speed and pitch-angle speed control with unrestricted ADRC.

From Figure 8, it can be seen that ADRC can realize the trajectory planning for the displacement of the hydraulic cylinder to achieve the displacement without overshooting, but due to the nonlinear relationship between the displacement of the hydraulic cylinder and the pitch angle, it will lead to the nonlinearity of the change of the pitch angle, and it is not possible to control the pitch angular velocity when there is no speed saturation limitation, which makes the pitch angular velocity exceeding the angular velocity limitation of 5 deg/s in the vicinity of 6–17 s and 25 s.

Experiments on the effect of displacement and velocity control with velocity and acceleration limited ADRC are carried out and the results are shown in Figure 9.

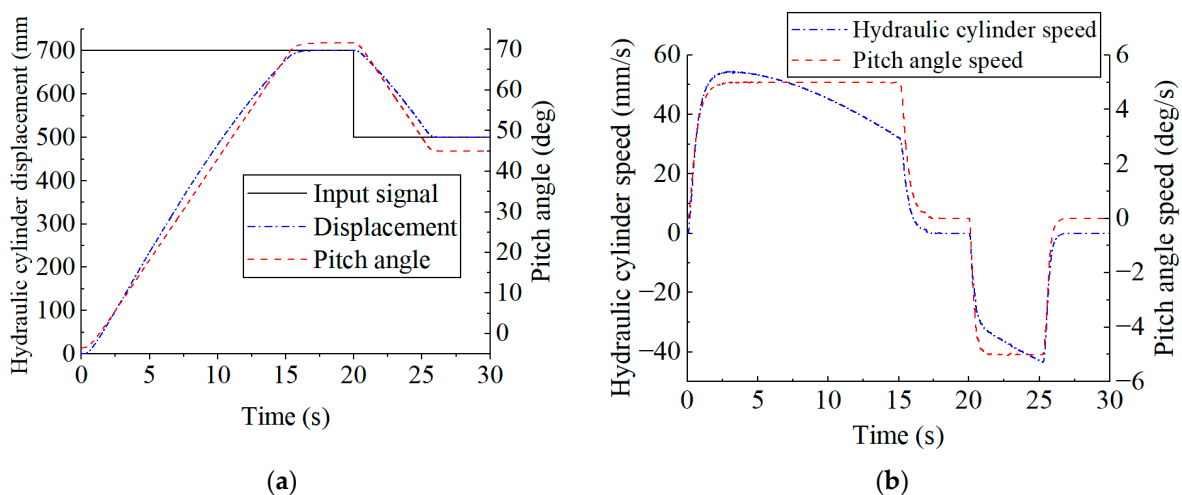


**Figure 9.** Displacement and velocity control with velocity and acceleration limited ADRC: (a) Hydraulic cylinder displacement and pitch-angle control with velocity and acceleration limited ADRC; (b) Hydraulic cylinder speed and pitch-angle speed control with velocity and acceleration limited ADRC.

After setting the pitch angular velocity and acceleration limits, not only can the hydraulic cylinder carry out better displacement and velocity planning, but also, through the nonlinearity of the hydraulic cylinder displacement and velocity, can be realized as the linearization of the pitch angle and the pitch angular velocity, to ensure that the pitch angular velocity stays within 5 deg/s.

### 6.2.2. Simulation Study of Acceleration Limiting Effect

Given a continuous step signal of hydraulic cylinder displacement, the paddle pitch angular acceleration response is observed with PID controller, without acceleration saturation limiting ADRC, and with acceleration saturation limiting ADRC, respectively, as shown in Figure 10.

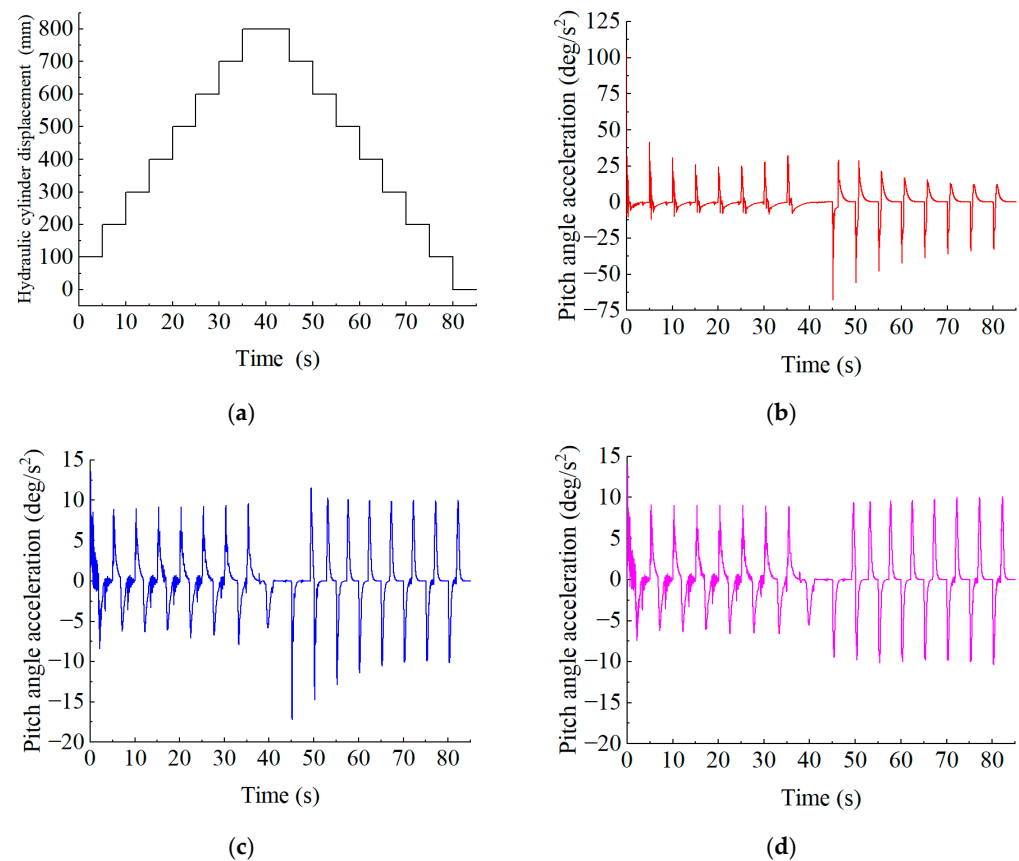


**Figure 10.** Acceleration response of continuous step signal of hydraulic cylinder displacement: (a) Continuous step signal of hydraulic cylinder displacement; (b) Acceleration response with PID; (c) Acceleration response with unrestricted ADRC; (d) Acceleration response with pitch angle velocity and acceleration limited ADRC.

From the figure, it can be seen that when using PID control, the pitch-angle acceleration is almost completely out of control, and the maximum pitch-angle acceleration can be up to 104 deg/s<sup>2</sup> for forward startup and 45 deg/s<sup>2</sup> for reverse startup, which is already far beyond the safety limiting condition of 20 deg/s<sup>2</sup> pitch-angle acceleration. The unrestricted ADRC acceleration is smaller compared to the PID as a whole, but there are some positions where the acceleration is larger, in the 20 deg/s<sup>2</sup> neighborhood. After setting the acceleration saturation limit, the peak paddle pitch angular acceleration is approximately equal regardless of forward and reverse startup, with an average peak value of 9 deg/s<sup>2</sup> for forward startup and 10 deg/s<sup>2</sup> for reverse startup, which can make the system startup smoother and more controllable.

### 6.2.3. Study of Controller Performance in the Presence of Wind Speed Disturbances

In order to verify the control effect when there is a wind speed disturbance, the pitch system is loaded with a disturbance at the actual wind speed, as shown in Figure 11.

Hydraulic cylinder extends 500 mm and retracts 50 mm when disturbed by wind speed. The effect is shown in Figure 12.

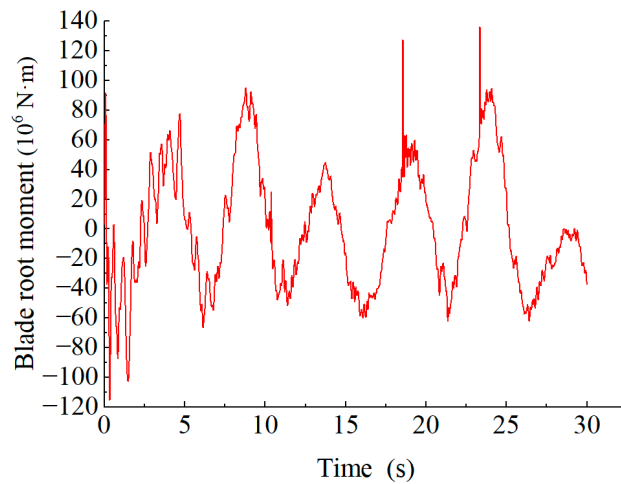


Figure 11. Wind speed disturbance signal.

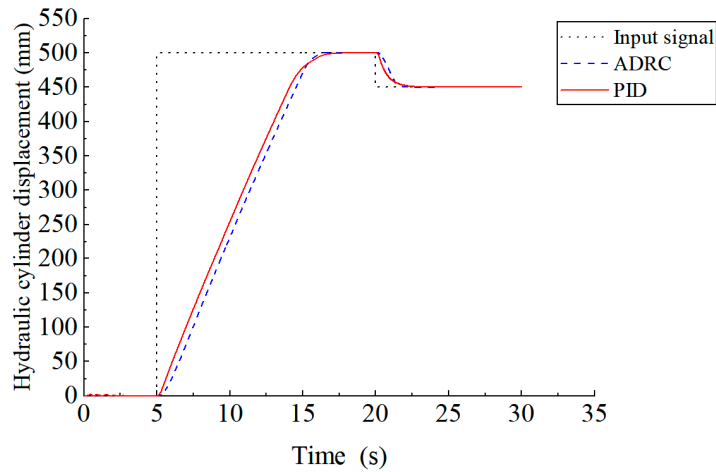


Figure 12. Hydraulic cylinder extends 500 mm and retracts 50 mm when disturbed by wind speed.

From the figure, it can be seen that the hydraulic cylinder extends 500 mm and retracts 50 mm when there is a wind speed perturbation; the operating speed PID is slightly faster compared to the ADRC, the speed exceeds the ADRC, and the ADRC transitions are smoother and smoother during the start and stop phases.

According to the pitch condition to add the load and carry out the pitch action, the PID and ADRC followings are shown in Figure 13.

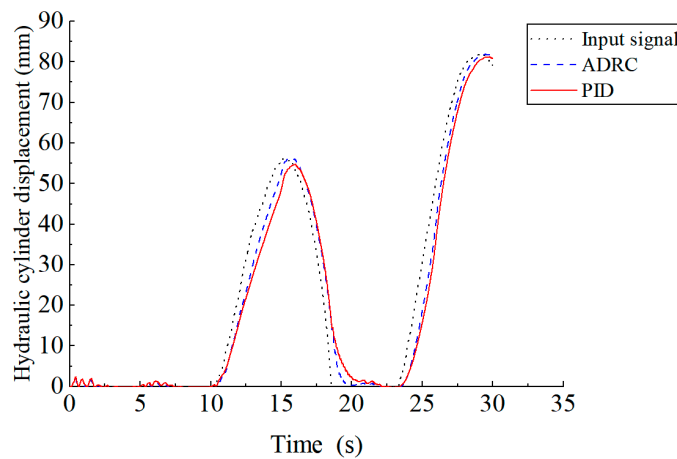
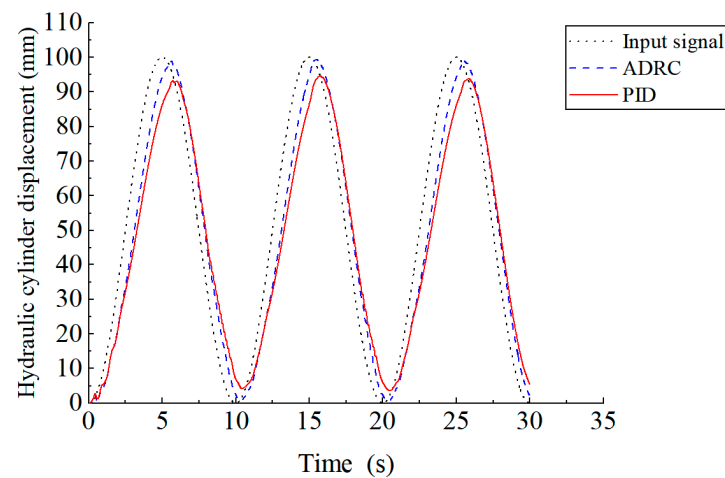


Figure 13. PID and ADRC following of pitch change maneuvers.

When there is a wind speed disturbance, the motion is performed according to a sinusoidal command with a frequency of 10 Hz and an amplitude of 100, and the effect is shown in Figure 14.



**Figure 14.** PID and ADRC following a 10 Hz sinusoidal signal.

The PID speed in the graph shows a first fast and then slow characteristic compared to ADRC, and does not reach 100 mm in amplitude tracking.

Through the above experiments, it is found that the ADRC with pitch angular velocity acceleration limitation improves the effect of pitch angular velocity and acceleration control significantly compared to the ADRC and PID without limitation and achieves the expected goal. When there is wind speed interference, the ADRC with speed and acceleration limitation has higher positional accuracy, smoother running speed, and stronger anti-interference ability compared with PID.

### 6.3. Physical Simulations Test

The experiment system for controlling pitch via an electro-hydraulic servo pump consists of a Moog MSCII controller, servo drive, servo motor, and hydraulic system. The controller utilizes sensors to monitor and gather real-time data on pressure, position, temperature, and other system parameters. The speed signal of the servo motor is output after processing according to the target displacement and actual displacement by the designed ADRC. Output the desired speed to the servo drive using EtherCAT communication. The drive rotates the servo motor through encoder cable. The hydraulic pump output flow is controlled to achieve hydraulic cylinder position control. The motion data of pitch angle are calculated according to the principle of pitch mechanism. The overall framework of the experimental platform is shown in Figure 15. The hydraulic component selection of the experimental platform is shown in Table 3.

**Table 3.** Hydraulic component selection.

| Serial number | Name                                    | Branding     |
|---------------|---|--------------|
| 1             | Accumulator                             | Li Ming      |
| 2             | Check valve                             | Hua De       |
| 3             | Relief valve                            | SUN          |
| 4             | Two-position two-way directional valves | SUN          |
| 5             | Throttle valve                          | SUN          |
| 6             | Temperature sensor                      | Zhu Hong     |
| 7             | Pressure sensors                        | Zhu Hong     |
| 8             | Displacement Sensor                     | Nanjing Xiju |

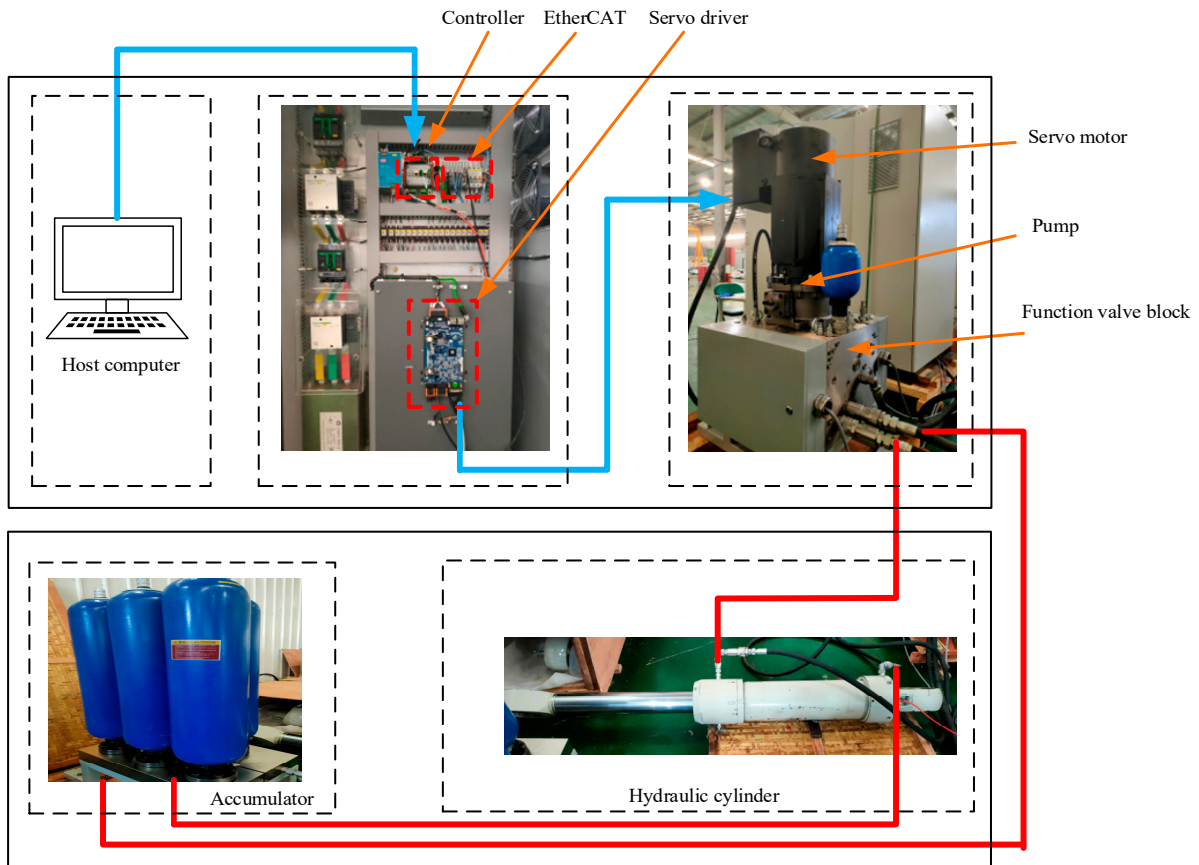


**Figure 15.** Overall framework of the experimental platform.

The test comprises the speed restriction test, acceleration limitation test, and sinusoidal response test of the system. Because of the inability to conduct experiments on wind turbines, the pitch angle and pitch-angle velocity are calculated according to the pitch mechanism and the hydraulic cylinder parameters.

### 6.3.1. Speed Limit Test

The speed limit test mainly verifies the speed limit effect of the designed controller. Enter step instructions with a hydraulic cylinder displacement of 800 mm to get an unlimited and limited ADRC control pitch-angle curve, as shown in Figure 16.

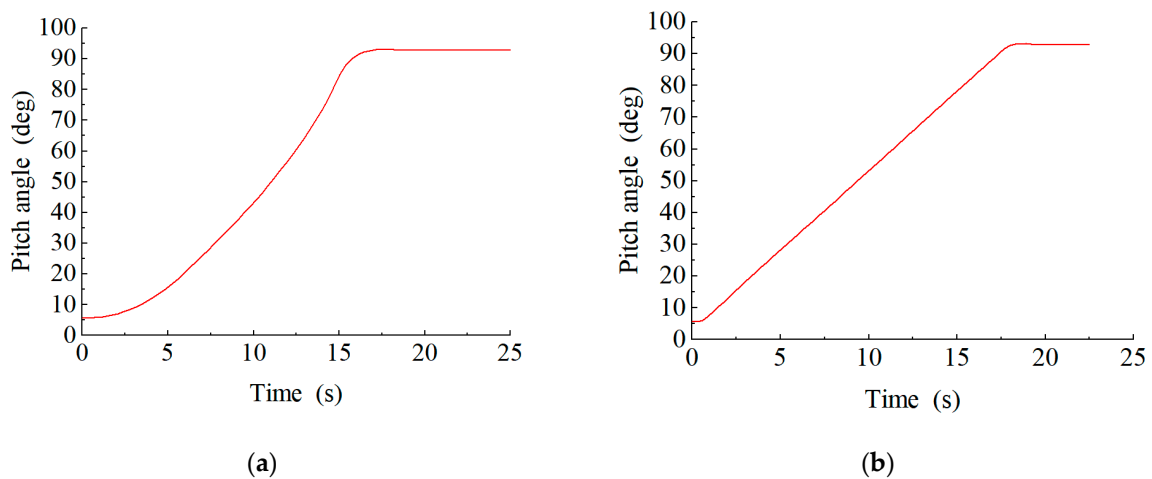


**Figure 16.** Unlimited and limited ADRC control pitch-angle curve. (a) Unlimited ADRC control pitch-angle curve, (b) Limited ADRC control pitch-angle curve.

By contrast, the nonlinear TD is designed to realize the nonlinear planning of the displacement of the hydraulic cylinder.

Enter step instructions with a hydraulic cylinder displacement of 800 mm to get an unlimited and limited ADRC control pitch-angle velocity curve, as shown in Figure 17.

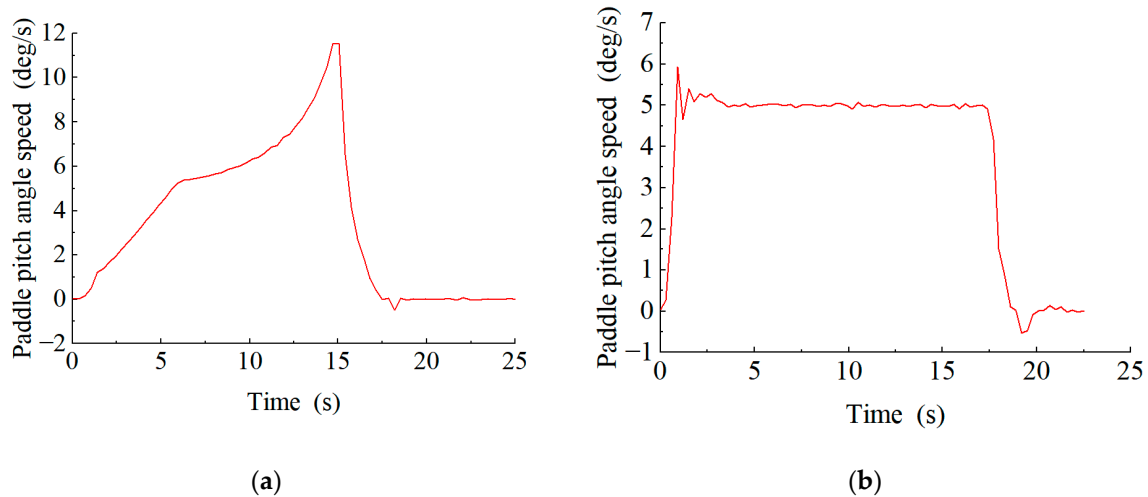


**Figure 17.** Unlimited and restricted ADRC control pitch-angle velocity curve. (a) Unlimited ADRC control pitch-angle velocity curve; (b) Limited ADRC control pitch-angle velocity curve.

By contrast, it can be seen that when the speed limit is not set, the pitch-angle speed change amplitude is larger, and the speed is uncontrollable. After setting the speed limit at 5 deg/s, the speed of the pitch angle quickly reaches the target value. During the pitch control, it is always controlled near the target value. Unlimited ADRC control pitch-angle speed peak is 11.6 deg/s. The limited ADRC control pitch-angle speed peak is 5.9 deg/s, and the limited ADRC control pitch-angle speed fluctuation is relatively smooth with higher safety. The pitch-angle velocity variance at 5–15 s unlimited ADRC is 1.85, and the limited ADRC angular velocity variance is 0.03. Using pitch-angle velocity variance as the velocity stability index, pitch angle stability increased by 98.38%. At the same time, it is also seen that the limited ADRC control pitch-angle velocity is partially overshoot during the start-up phase. This may be related to nonlinear factors not considered in part of the experimental platform and the parameters selected by the controller.

### 6.3.2. Acceleration Limited Tests

The acceleration limited test assesses the ability of the planned TD to achieve acceleration magnitude limitation when the hydraulic cylinder is initiated from various positions. Enter the continuous step command for hydraulic cylinder displacement to obtain the pitch-angle acceleration curve depicted in Figure 18.

As can be seen from Figure 18b, due to the nonlinear properties of the pitch mechanism, when using PID control, hydraulic cylinder acceleration is always the maximum response acceleration of the hydraulic system. After the pitch mechanism, it will make the pitch-angle acceleration change more. The maximum acceleration of the pitch angle is 66 deg/s<sup>2</sup>, which is prone to hazard. As can be seen in Figure 18c, the maximum pitch angle is more than 20 deg/s<sup>2</sup>, the peak pitch angle is 23 deg/s<sup>2</sup>; as can be seen in Figure 18d, ADRC with an acceleration limit can limit the pitch-angle acceleration to the target value. After the above comparison analysis, it can be seen that setting the acceleration limit in the nonlinear tracking differential can make the pitch-angle acceleration peak smoother, so that the pitch-angle acceleration is always stable in the set safety value, and can improve the safety of the pitch control system.

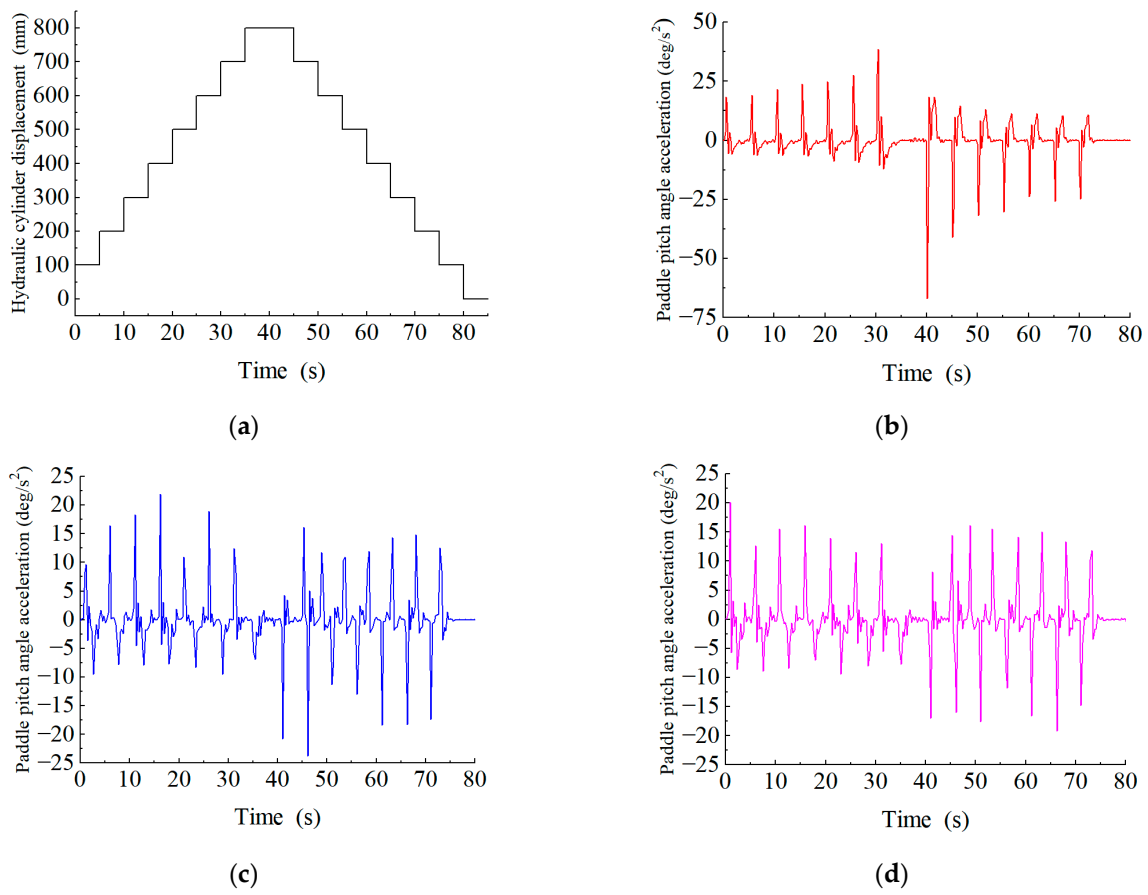


**Figure 18.** Continuous step signal and pitch-angle acceleration response curve. (a) Continuous step command signal; (b) pitch-angle acceleration curve with PID control; (c) no acceleration limit ADRC pitch-angle acceleration curve; (d) acceleration limit ADRC pitch-angle acceleration curve.

### 6.3.3. Sinusoidal Response Test

The main purpose of the sine step response test is to test the sine signal follow ability of the system. The input amplitude is 50 mm, the frequency is 0.05 Hz of the sine signal instruction, and the PID and the speed and acceleration limited ADRC to control the hydraulic cylinder response curves is obtained, as shown in Figure 19.

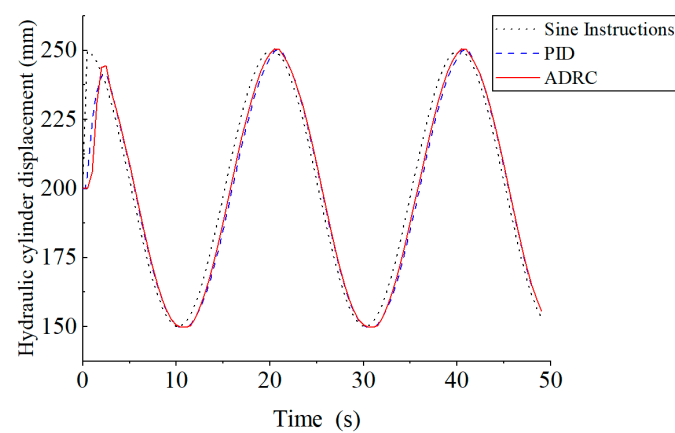


**Figure 19.** Sine response curves for PID and ADRC control.

The curves in Figure 19 shows that, after setting the speed and acceleration limits, the designed ADRC can still track sine signals quickly and without amplitude attenuation. In a sine cycle of 10–30 s, with 0.5 s as the sampling period, the displacement variance

between the PID and the target signal is 45.26. The displacement variance between the designed ADRC and the target signal is 2.67. The designed ADRC improved by 94.1% compared to the PID position accuracy when evaluated with displacement variance.

## 7. Conclusions

Through the theoretical analysis method, the nonlinear relationship expression between pitch angle and hydraulic cylinder displacement is derived; the modeling analysis method is used to obtain the calculation formula of  $b_0$  of the pump-controlled pitch system, and the key parameters of the self-resistant controller are determined; the stability of the controller parameters is proved through stability analysis and simulation analysis, and the design of the self-resistant controller with pitch-angle speed and acceleration limitation is accomplished.

A joint simulation platform of AMESim and MATLAB and a physical experiment platform of electro-hydraulic servo-pump-controlled pitch control are built, and the effectiveness of the proposed control method is verified through simulation and experiment. The results show that compared with the unrestricted ADRC and PID, the velocity-acceleration-limited ADRC can smoothen the startup process and improve the safety of the system with better position control accuracy and anti-jamming ability while realizing the objectives of limiting the angular velocity of the paddle blade to 5 deg/s and the angular acceleration to 20 deg/s<sup>2</sup>.

The key components of wind turbines, such as the blades, are subjected to both wind load and control load for a long time, and are prone to fatigue damage that affects the reliability and life of the turbine, which is not explored in depth in this paper. In the next step, we will quantitatively evaluate the load reduction effect of the designed ADRC system with limited pitch angular velocity and angular acceleration by a combination of simulation and experiment. By combining structural health monitoring and ADRC, we can more comprehensively evaluate the actual effectiveness of the control system, optimize the control strategy, and extend the service life of the wind turbine. Integration of servo-pump-controlled pitch technology with the turbine condition monitoring system realizes more intelligent and networked turbine monitoring, operation, and maintenance.

**Author Contributions:** Conceptualization, T.Z. and H.Y.; methodology, B.Y. and P.X.; experiment, H.Y. and X.L.; software, X.L. and J.L.; investigation, R.L. and J.L.; writing—original draft preparation, T.Z.; writing—review and editing, B.Y.; analysis, P.X. and R.L.; project administration, C.A.; funding acquisition, C.A. All authors have read and agreed to the published version of the manuscript.

**Funding:** This research was funded by the Science and Technology Research Program of Higher Education Institutions in Hebei Province (CXY2024034), the Natural Science Foundation of Xinjiang Uygur Autonomous Region (2022D01A244), Autonomous Region Colleges and Universities Research Program (XJEDU2024P087), the Basic Research Funds for Universities of Xinjiang (XJEDU2023P138).

**Data Availability Statement:** Data are contained within the article.

**Conflicts of Interest:** Author Xiaoxiang Lou was employed by Ningbo Anson CNC Technique Co., Ltd., Ruilin Li and Jianchen Li were employed by Shenzhen Inovance Technology Co., Ltd. The remaining authors declare that the research was conducted in the absence of any commercial or financial relationships that could be construed as a potential conflict of interest.

## References

1. Chen, W.T.; Wang, X.Y.; Zhang, F.S.; Liu, H.W.; Lin, Y.G. Review of the application of hydraulic technology in wind turbine. *Wind Energy* **2020**, *23*, 1495–1522. [[CrossRef](#)]
2. Gao, B.W.; Shen, W.; Zheng, L.T.; Zhang, W.; Zhao, H.J. A Review of Key Technologies for Friction Nonlinearity in an Electro-Hydraulic Servo System. *Machines* **2022**, *10*, 568. [[CrossRef](#)]
3. Zhou, M.L.; Gao, W.; Yang, Z.G.; Tian, Y.T. High Precise Fuzzy Control for Piezoelectric Direct Drive Electro-Hydraulic Servo Valve. *J. Adv. Mech. Des. Syst. Manuf.* **2012**, *6*, 1154–1167. [[CrossRef](#)]
4. Zhu, J.; Yang, X.; Xie, G.; Cao, Z. Design and damping performance analysis of a multistage meandering hybrid valved magnetorheological damper. *Phys. Scr.* **2024**, *99*, 045517. [[CrossRef](#)]

5. Yang, S.; Yao, J.; Wang, P.; Zhang, P.; Wei, T.; Li, D. A novel Dual-Magnetic circuit actuated Fast-Switching valve with Multi-Stage excitation control algorithm. *Measurement* **2024**, *230*, 114483. [[CrossRef](#)]
6. Dindorf, R. Dynamic Modeling and Simulation of a Discrete Incremental Hydraulic Positioning System Controlled by Binary Valves. *Appl. Sci.* **2024**, *14*, 2973. [[CrossRef](#)]
7. Yan, G.S.; Jin, Z.L.; Zhang, T.G.; Zhang, C.; Ai, C.; Chen, G.X. Exploring the Essence of Servo Pump Control. *Processes* **2022**, *10*, 786. [[CrossRef](#)]
8. Zhang, T.G.; Chen, G.X.; Yan, G.S.; Zhang, C.; Li, Y.; Ai, C. Research on the Nonlinear Characteristic of Flow in the Electro-Hydraulic Servo Pump Control System. *Processes* **2021**, *9*, 814. [[CrossRef](#)]
9. Li, R.; Zhang, Y.; Feng, Z.; Xu, J.; Wu, X.; Liu, M.; Xia, Y.; Sun, Q.; Yuan, W. Review of the Progress of Energy Saving of Hydraulic Control Systems. *Processes* **2023**, *11*, 3304. [[CrossRef](#)]
10. Ruqi, D.; Hongzhi, Y.; Min, C.; Gang, L.; Bing, X. The design and analysis of a hydro-pneumatic energy storage closed-circuit pump control system with a four-chamber cylinder. *J. Energy Storage* **2024**, *79*, 110076.
11. Wang, H.; Zhang, Y.; An, Z.; Liu, R. An Energy-Efficient Adaptive Speed-Regulating Method for Pump-Controlled Motor Hydrostatic Drive Powertrains. *Processes* **2023**, *12*, 25. [[CrossRef](#)]
12. Helian, B.; Chen, Z.; Yao, B. Precision Motion Control of a Servomotor-Pump Direct-Drive Electrohydraulic System with a Nonlinear Pump Flow Mapping. *IEEE Trans. Ind. Electron.* **2020**, *67*, 8638–8648. [[CrossRef](#)]
13. Yao, J.Y.; Deng, W.X.; Jiao, Z.X. RISE-Based Adaptive Control of Hydraulic Systems with Asymptotic Tracking. *IEEE Trans. Autom. Sci. Eng.* **2017**, *14*, 1524–1531. [[CrossRef](#)]
14. Yang, M.K.; Chen, G.X.; Lu, J.X.; Yu, C.; Yan, G.S.; Ai, C.; Li, Y.W. Research on Energy Transmission Mechanism of the Electro-Hydraulic Servo Pump Control System. *Energies* **2021**, *14*, 4869. [[CrossRef](#)]
15. Liu, R.S.; Wang, Z.K.; Jia, P.S.; Yan, G.S.; Zhang, T.G.; Jia, C.Y.; Chen, G.X. Research on Pressure Control of an Electro-Hydraulic Servo System Based on Sliding-Mode Variable-Structure Direct Torque Control. *Processes* **2023**, *11*, 92. [[CrossRef](#)]
16. Yan, G.S.; Jin, Z.L.; Yang, M.K.; Yao, B. The Thermal Balance Temperature Field of the Electro-Hydraulic Servo Pump Control System. *Energies* **2021**, *14*, 1364. [[CrossRef](#)]
17. Sun, W.C.; Pan, H.H.; Gao, H.J. Filter-Based Adaptive Vibration Control for Active Vehicle Suspensions with Electrohydraulic Actuators. *IEEE Trans. Veh. Technol.* **2016**, *65*, 4619–4626. [[CrossRef](#)]
18. Wang, B.L.; Cai, Y.; Song, J.C.; Liang, Q.K.; Ren, G.G. Enhanced reduced-order extended state observers-based position tracking error constraint control of a pump-controlled hydraulic system via multiparameter singular perturbation theory. *Control Eng. Pract.* **2024**, *142*, 12. [[CrossRef](#)]
19. Wang, B.L.; Cai, Y.; Song, J.C.; Liang, Q.K. A Singular Perturbation Theory-Based Composite Control Design for a Pump-Controlled Hydraulic Actuator with Position Tracking Error Constraint. *Actuators* **2023**, *12*, 265. [[CrossRef](#)]
20. Imam, A.; Tolba, M.; Sepehri, N. A Comparative Study of Two Common Pump-Controlled Hydraulic Circuits for Single-Rod Actuators. *Actuators* **2023**, *12*, 193. [[CrossRef](#)]
21. Wang, H.S.; Zhang, Y.B.; Li, G.Q.; Liu, R.S.; Zhou, X. Design and Control of an Energy-Efficient Speed Regulating Method for Pump-Controlled Motor System under Negative Loads. *Machines* **2023**, *11*, 437. [[CrossRef](#)]
22. Nguyen, M.H.; Ahn, K.K. Output Feedback Robust Tracking Control for a Variable-Speed Pump-Controlled Hydraulic System Subject to Mismatched Uncertainties. *Mathematics* **2023**, *11*, 1783. [[CrossRef](#)]
23. Yang, M.K.; Yan, G.S.; Zhang, Y.H.; Zhang, T.G.; Ai, C. Research on high efficiency and high dynamic optimal matching of the electro-hydraulic servo pump control system based on NSGA-II. *Heliyon* **2023**, *9*, e13805. [[CrossRef](#)]
24. Singh, V.P.; Pandey, A.K.; Dasgupta, K. Steady-state performance investigation of closed-circuit hydrostatic drive using variable displacement pump and variable displacement motor. *Proc. Inst. Mech. Eng. Part E-J. Process Mech. Eng.* **2021**, *235*, 249–258. [[CrossRef](#)]
25. Anwar, M.N.; Pan, S.; Ghosh, S. PI controller design for pitch control of large wind turbine generator. In Proceedings of the International Conference on Energy, Power and Environment: Towards Sustainable Growth (ICEPE), Shillong, India, 12–13 June 2016.
26. Farong, K.; Yawei, G.; Qiangqiang, J.; Xianlong, P.; Xing, W. LQG control of active suspension based on adaptive road surface level. *J. Vib. Shock*. **2020**, *39*, 30–37. [[CrossRef](#)]
27. Wu, X.; Su, R.; Lu, C.F.; Rui, X.M. Internal Leakage Detection for Wind Turbine Hydraulic Pitching System with Computationally Efficient Adaptive Asymmetric SVM. In Proceedings of the 34th Chinese Control Conference (CCC), Hangzhou, China, 28–30 July 2015; pp. 6126–6130.
28. Gu, Y.; Yin, X.; Liu, H.; Li, W.; Xu, Q. Adaptive backstepping pitch control of direct drive hydraulic pump-controlled-motor system. *Acta Energetica Solaris Sinica*. **2016**, *37*, 3219–3225.
29. Li, B.; Zhang, Z.-Q.; Yu, H.-H.; Zhao, R.; Zhang, T.-G.; Yan, G.-S.; Ai, C. Study on Variable Pitch Control of Pump Controlled Hydraulic System of Wind Turbine. *Chin. Hydraul. Pneum.* **2023**, *47*, 27–35.
30. Bilal, H.; Yin, B.Q.; Aslam, M.S.; Anjum, Z.; Rohra, A.; Wang, Y.Z. A practical study of active disturbance rejection control for rotary flexible joint robot manipulator. *Soft Comput.* **2023**, *27*, 4987–5001. [[CrossRef](#)]
31. Yao, J.Y.; Deng, W.X. Active Disturbance Rejection Adaptive Control of Hydraulic Servo Systems. *IEEE Trans. Ind. Electron.* **2017**, *64*, 8023–8032. [[CrossRef](#)]

32. Xue, W.C.; Bai, W.Y.; Yang, S.; Song, K.; Huang, Y.; Xie, H. ADRC With Adaptive Extended State Observer and its Application to Air-Fuel Ratio Control in Gasoline Engines. *IEEE Trans. Ind. Electron.* **2015**, *62*, 5847–5857. [[CrossRef](#)]
33. Liang, Z.Z.; Zhu, G.B. A Novel Extended State Observer for Output Tracking of MIMO Systems with Mismatched Uncertainty. *IEEE Trans. Autom. Control* **2018**, *63*, 211–218.

**Disclaimer/Publisher’s Note:** The statements, opinions and data contained in all publications are solely those of the individual author(s) and contributor(s) and not of MDPI and/or the editor(s). MDPI and/or the editor(s) disclaim responsibility for any injury to people or property resulting from any ideas, methods, instructions or products referred to in the content.